Low Temperature Physics/Fizika Nizkikh Temperatur, 2012, v. 38, No. 11, pp. 1306–1312

Method of trial distribution function for quantum turbulence

Sergey K. Nemirovskii

Institute of Thermophysics, Academy of Sciences, Novosibirsk 630090, Russia
Novosibirsk State University, Novosibirsk, Russia
E-mail: nemir@itp.nsc.ru

Received June 13, 2012

Studying quantum turbulence the necessity of calculation the various characteristics of the vortex tangle (VT) appears. Some of "crude" quantities can be expressed directly via the total length of vortex lines (per unit of volume) or the vortex line density $\mathcal{L}(t)$ and the structure parameters of the VT. Other more “subtle” quantities require knowledge of the vortex line configurations $\{\mathbf{s}(\xi,t)\}$. Usually, the corresponding calculations are carried out with the use of more or less truthful speculations concerning arrangement of the VT. In this paper we review other way to solution of this problem. It is based on the trial distribution functional (TDF) in space of vortex loop configurations. The TDF is constructed on the basis of well established properties of the vortex tangle. It is designed to calculate various averages taken over stochastic vortex loop configurations. In this paper we also review several applications of the use this model to calculate some important characteristics of the vortex tangle. In particular we discussed the average superfluid mass current J induced by vortices and its dynamics. We also describe the diffusion-like processes in the nonuniform vortex tangle and propagation of turbulent fronts.

PACS: *67.25.dk* Vortices and turbulence;
47.37.+q Hydrodynamic aspects of superfluidity; quantum fluids;
05.20.–y Classical statistical mechanics.

Keywords: superfluidity, vortices, quantum turbulence.

1. Introduction and scientific background

Quantum turbulence studying phenomenon is related to appearance of one dimensional quantized vortex filaments (vortex tangles) in flowing quantum liquids ^{3}He and ^{4}He and also Bose–Einstein gases. The presence of vortex tangle essentially influences various physical properties of the quantum fluids (see, e.g., recent reviews [1,2]). To study the corresponding properties we need to evaluate characteristics related to presence of vortex tangles. Some of characteristics can be expressed in terms of the total length of vortex lines (per unit of volume) or the vortex line density (VLD) $\mathcal{L}(t)$ and of the structure parameters of the vortex tangle (VT) known from the direct numerical simulations by Schwarz [3]. Knowledge of these quantities allows to calculate some of hydrodynamic characteristics of superfluid turbulent He II such as a mutual friction, sound attenuation etc. Meanwhile there exist many other physical quantities, which should be evaluated on the basis of the more detailed description of the vortex filaments, rather than the VLD $\mathcal{L}(t)$ and of the structure parameters of the VT. The relevant distribution function should be obtained from appropriate stochastic theory of chaotic vortex filaments. Of course, the most straightforward way to develop theory is to study stochastic dynamics of vortex filaments on the base of equations of motion with some source of chaos. The final aim of such theory is to find the probability functional $\mathcal{P}(\{\mathbf{s}(\xi)\})$ for the vortex filaments configurations $\{\mathbf{s}(\xi,t)\}$ (in our paper we apply widely-used notations (see, e.g., [4]). Knowing of $\mathcal{P}(\{\mathbf{s}(\xi)\})$ allows us to calculate any average depending on the presence of VT. However due to extremely involved dynamics of vortex lines this way seems to be almost hopeless. Thus, a necessity of a developing an advanced phenomenological approach appeared.

In the present paper we review a variant of such approach and give several examples of important physical applications. The main idea and the main strategy are the following. Although the phenomenological theory of the superfluid turbulence deals with macroscopic characteristics of the vortex tangle, it conveys the rich information concerning the *instantaneous* structure of the vortex tangle. Namely we know that the VT consists of the closed loops labeled by $\mathbf{s}_j(\xi)$, uniformly distributed in space and having the total length $\mathcal{L}(t)$ per unit of volume.

From acoustical experiments it follows that filaments are distributed in anisotropic manner and quantitative characteristics of this anisotropy can be expressed by some structure parameters (see [3–5]). Beside this usual anisotropy there is more subtle anisotropy connected with averaged polarization of the vortex loops. Furthermore there are some proofs that the averaged curvature of the vortex lines is proportional to the inverse interline space and coefficient of this proportionality (which is of order of unit) was obtained in numerical simulations made by Schwarz [3].

The master idea of the proposal, which we are reviewing here, is to construct a trial distribution function (TDF) in the space of the vortex loops of the most general form which satisfies to all of the properties of the VT introduced above. We assume that this trial distribution function will enable us to calculate any physical quantities due to the VT. In the paper we describe some properties of the VT, following from the trial distribution function. Namely we study the average hydrodynamic impulse (or Lamb impulse) J_V in the counterflowing superfluid turbulent He II. We also describe the diffusion-like processes in the nonuniform vortex tangle and propagation of turbulent fronts.

2. Constructing of the trial distribution function

According to general prescriptions the average of any quantity $\langle \mathcal{B}(\{\mathbf{s}_j(\xi_j)\})\rangle$ depending on vortex loop configurations is given by

$$\langle \mathcal{B}(\{\mathbf{s}_j(\xi_j)\})\rangle = \sum_{\{\mathbf{s}_j(\xi_j)\}} \mathcal{B}(\{\mathbf{s}_j(\xi_j)\})\mathcal{P}(\{\mathbf{s}_j(\xi_j)\}). \quad (1)$$

Here $\mathcal{P}(\{\mathbf{s}_j(\xi_j)\})$ is a probability of the vortex tangle to have a particular configuration $\{\mathbf{s}_j(\xi_j)\}$. Index j distinguishes different loops. The meaning of summation over all vortex loop configurations $\sum_{\{\mathbf{s}_j(\xi_j)\}}$ in formula (1) will be clear from further presentation. We put the usual in the statistical physics supposition that all configuration corresponding to the same macroscopic state have equal probabilities. Thus the probability $\mathcal{P}(\{\mathbf{s}_j(\xi_j)\})$ for vortex tangle to have a particular configuration $\{\mathbf{s}_j(\xi_j)\}$ should be proportional to $1/N_{\text{allowed}}$, where N_{allowed} is the number of allowed configurations, of course infinite

$$\mathcal{P}(\{\mathbf{s}_j(\xi_j)\}) \propto \frac{1}{N_{\text{allowed}}}. \quad (2)$$

Under term “allowed configurations” N_{allowed} we mean only the configurations that will lead to the correct values for all average quantities known from experiment and numerical simulations. Formally it can be expressed as a path integral in space of three-dimensional (closed) curves supplemented with some constrains connected to properties of the VT:

$$N_{\text{allowed}} \propto \prod_j \int \mathcal{D}\{\mathbf{s}_j(\xi)\} \times \text{constraints}\,\{\mathbf{s}_j(\xi)\}. \quad (3)$$

The constraints entering this relation are expressed by delta functions expressing fixed properties of the VT. The first, main constrain $\delta((\mathbf{s}'_j(\xi))^2 - 1)$ (the label variable ξ is the arc length) expresses condition of connectivity, the close along the line points cannot run away from each other. However this condition will lead to not tractable theory. We will use a trick known from the theory of polymer chains (see, e.g., [6]), namely we will relax rigorous condition and change delta function by continuous (Gaussian) distribution of the link length with the same value of integral. This trick leads to the following expression for number of way:

$$N_{\text{allowed}} \propto \prod_j \int \mathcal{D}\{\mathbf{s}_j(\xi)\} \exp(-\lambda_1 \int_0^{\mathcal{L}} |\mathbf{s}'|^2 \, d\xi). \quad (4)$$

In the same manner we are able to introduce and treat other constrains connected to the known properties of the VT structure. The detailed calculations are exposed in paper of the author [7], now we write down the final expression for probability of configurations

$$N_{\text{allowed}} \propto \int \mathcal{D}\{\mathbf{s}(\xi)\} \exp\left(-\mathcal{H}\{\mathbf{s}(\xi)\}\right). \quad (5)$$

Here $\mathbf{s}(\kappa)$ is one-dimensional Fourier transform of variable $\mathbf{s}(\xi)$ and Hamiltonian $\mathcal{H}\{\mathbf{s}(\kappa)\}$ is a quadratic form of the components of the vector variable $\mathbf{s}(\kappa)$

$$\mathcal{H}\{\mathbf{s}(\xi)\} = \int_0^l \int_0^l \mathbf{s}'^{\alpha}(\xi_1, t)\Lambda^{\alpha\beta}(\xi_1 - \xi_2)\mathbf{s}'^{\beta}(\xi_2, t) d\xi_1 d\xi_2. \quad (6)$$

The typical form of function $\Lambda^{\alpha\beta}(\xi, \xi')$ is a smoothed δ function, of a Mexican hat shape with width equal to ξ_0. Note that the case $\Lambda^{\alpha\beta}(\xi_1 - \xi_2) = \delta_{\alpha\beta}\delta(\xi_1 - \xi_2)$ corresponds to the classical Wiener distribution. In practice to calculate various averages it is convenient to work with the characteristic (generating) functional (CF) which is defined as a following average:

$$W(\{\mathbf{P}_j(\xi_j)\}) = \left\langle \exp\left(i \sum_j \int_0^{L_j} \mathbf{P}_j(\xi_j)\mathbf{s}'_j(\xi_j)\, d\xi_j \right) \right\rangle. \quad (7)$$

Due to that our Hamiltonian (6) is a quadratic form (in $\mathbf{s}(\kappa)$) and, consequently, the trial distribution function is a Gaussian one, calculation of the CF can be made by accomplishing the full square procedure to give a result

$$W_{\text{Gauss}}(\{\mathbf{P}(\xi,t)\}) =$$
$$= \exp\left\{-\int_0^l \int_0^l \mathbf{P}^{\alpha}(\xi_1) N^{\alpha\beta}(\xi_1-\xi_2)\mathbf{P}^{\beta}(\xi_2)d\xi_1 d\xi_2\right\}. \quad (8)$$

The function $N^{\alpha\beta}(\xi_1-\xi_2)$ should also be a smoothed δ function of a Mexican hat shape with width equal to ξ_0. The explicit form of them is written down in [7]. The matrix form of $N^{\alpha\beta}$ reflects anisotropy of the counterflowing quantum fluid.

Thus we reached the put goal and have written the expression for trial distribution function which, we repeat, enables us to calculate any averaged of the vortex filament configuration. For instance calculating some of the correlation functions we are able to describe a typical shape of the averaged curve. It is sketched out in Fig. 1. It is remarkable that the TDF has a Gaussian form; it facilitates any practical calculations. For this reason, the stated above approach, is usually referred to as the Gaussian model.

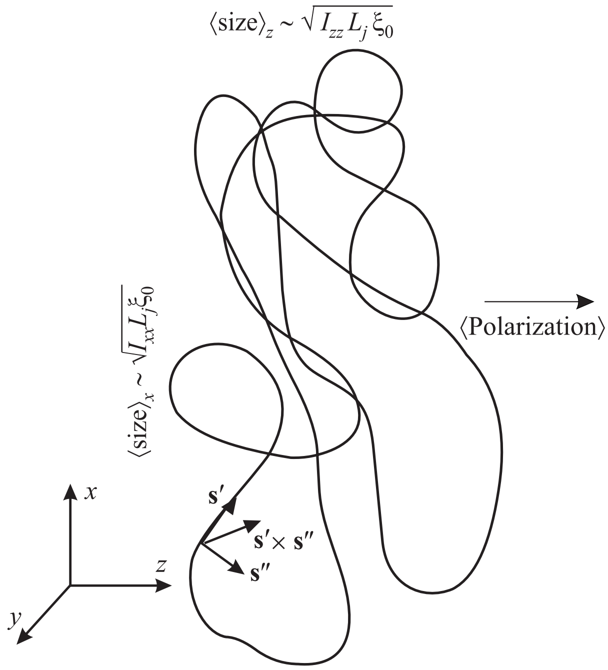

Fig. 1. A snapshot of the averaged vortex loop obtained from analysis of the statistical properties. Position of the vortex line element is described as $\mathbf{s}_j(\xi_j)$, where ξ_j is arc length, $\mathbf{s}'_j(\xi_j) = d\mathbf{s}_j(\xi_j)/d\xi_j$ is a tangent vector, unit vector along the vortex line; $\mathbf{s}''_j(\xi_j) = d^2\mathbf{s}_j(\xi_j)/d\xi_j^2$ is the local curvature vector; vector production $\mathbf{s}'_j(\xi_j)\times\mathbf{s}''_j(\xi_j)$ is binormal which is responsible for mutual orientation of the tangent vector and vector of curvature. Close $(\Delta\xi \ll R,$ where R is the mean curvature) parts of the line are separated in 3D space by distance $\Delta\xi$. The distant part $(R \ll \Delta\xi)$ are separated in 3D space by distance $\sqrt{2\pi R\Delta\xi}$ (with correction due to the closeness). The latter property reflects a random walk structure of the vortex loops. As a whole the loop is not isotropic having a "pancake" form. In addition it has a total polarization $\langle\int \mathbf{s}'_j(\xi_j)\times\mathbf{s}''_j(\xi_j)d\xi_j\rangle$ forcing the loop to drift along vector $\mathbf{V}_n$ and to produce nonzero superfluid mass current in *z* direction.

3. Hydrodynamic impulse of vortex tangle

3.1. Static properties

As an one more illustration to the developed theory we discuss hydrodynamic impulse (Lamb impulse) of the vortex tangle $\mathbf{J}_V$, which is defined as

$$\mathbf{J}_V = \langle\frac{\rho_s\tilde{\kappa}}{2}\sum_j\int \mathbf{s}_j(\xi_j)\times\mathbf{s}'_j(\xi_j)\,d\xi_j\rangle. \quad (9)$$

The quantity $\mathbf{J}_V$ is closely related to momentum of fluid (see [8]). Let us evaluate the Lamb impulse in the counterflowing helium II. The averaged $\langle\mathbf{s}_j(\xi_j)\times\mathbf{s}'_j(\xi_j)\rangle$ is immediately evaluated by use of CF (8) to give the following result (see [9]):

$$\mathbf{J}_V = -\left[\frac{\rho\tilde{\kappa} I_l \alpha_v}{\rho_n c_2^2 \beta_v}\right]\rho_s \mathbf{V}_s. \quad (10)$$

Here α_v and β_v are the coefficient of the Vinen equation (see, e.g., [4]). Quantity I_l, the so-called structure parameter was introduced by Schwarz to describe polarization of vortex loops in the direction of counterflow $\mathbf{V}_{ns}$. Note that the coefficient includes no fitting parameters but only characteristics known from the phenomenological theory (see [3]). Relation (10) shows that the vortex tangle induces the superfluid current directed against the external superfluid current. It should be expected since there is some preferable polarization of the vortex loops. In the experiments this additional superfluid current should display itself as suppression of the superfluid density $\Delta\rho_s$, which is the coefficient before $\mathbf{V}_s$ in (10). This effect is 3D analog to the famous Kosterlitz–Thouless effect except of that distribution of the vortex lines is not calculated but is obtained appealing to the experimental data.

Since superfluid density enters an expression for second sound velocity, it seems attractive to detect it using transverse second sound testing. To do it we have firstly to evaluate transverse change of the ρ_s and, secondly, to develop the theory to match it to nonstationary case. The general theory asserts that if one applies a harmonic external second sound field, the suppression of superfluid density becomes the function of frequency ω of the following form:

$$\Delta\rho_s^{\perp}(\omega) = \left(\frac{\delta\mathbf{J}_V^{\perp}}{\delta\mathbf{V}_s^{\perp}}\right)_{\text{transv}} \frac{1}{1+i\omega\tau_J}. \quad (11)$$

Here transverse $(\delta\mathbf{J}_V^{\perp}/\delta\mathbf{V}_s^{\perp})_{\text{transv}}$ is half of the one given by Eq. (10) (details are given in [9]). The quantity τ_J is the time of relaxation of the superfluid current J_V, which is to be found from dynamical consideration. First, we have to derive $d\mathbf{J}_V^{\perp}/dt$ with help of the equation of motion of the vortex line elements and, second, to evaluate various averaged appearing in right-hand side function we obtain the following final result for change of the second sound velocity. Performing all of described procedures one obtains that the relative change $\Delta u_2 / u_2$ of the second sound velocity is given by

$$\frac{\Delta u_2}{u_2} = -f(T)\frac{\mathbf{V}_{ns}^4}{\omega^2}. \tag{12}$$

Here the function $f(T)$ is composed of the structure parameters of the vortex tangle (see [3])

$$f(T) = \frac{4\rho\tilde{\kappa}\, I_l^2 \alpha^2 (1 - I_{\|})^2}{\rho_n c_2^4 \beta^3}. \tag{13}$$

Decreasing of the second sound velocity in the counterflowing He II has been really observed about two decades ago by Vidal with coauthors [10]. Let us compare our result (12) with the Vidal's experiment. Using the data on the structure parameters one obtains that, e.g., for the temperatures 1.44 K the value of function $f(T)$ is about 620 s^2/cm^4. Taking the frequency $\omega = 4.3$ rad/s, used in [10], and $V_{ns} = 2$ cm/s one obtains that $\Delta u_2 / u_2 \approx 4 \cdot 10^{-4}$, which is very close to the observed value.

3.2. Dynamics of the Lamb impulse

The rate of change of the Lamb impulse can be calculated by the direct differentiation the quantity (9) with respect to time assigning the line elements positions to depend on t $\mathbf{s}_j(\xi_j) \to \mathbf{s}_j(\xi_j, t)$:

$$\frac{d\mathbf{J}_V}{dt} = \rho_s \tilde{\kappa} \sum_j \int \left\langle \dot{\mathbf{s}}_j(\xi_j, t) \times \mathbf{s}'(\xi_j) \right\rangle d\xi_j. \tag{14}$$

Here $\langle ... \rangle$ imply an averaging over the vortex loop configuration. Using the equation of motion of the vortex line discussed in details, e.g., in [4], we arrive at

$$\frac{d\mathbf{J}_V}{dt} = -\rho_s \tilde{\kappa} \sum_j \int \left\langle \mathbf{s}'_j(\xi_j) \times \left(\mathbf{V}_s + \mathbf{V}_i + \alpha \mathbf{s}'_j \times (\mathbf{V}_{ns} - \mathbf{V}_i) \right) \right\rangle d\xi_j. \tag{15}$$

Here the quantity α is the friction coefficient (see, e.g., [3]), $\mathbf{V}_s$ is the external superfluid velocity and $\mathbf{V}_i$ is the self-induced velocity of the line elements induced by the whole vortex filaments configuration and expressed by the Biot–Savart law. Note that the first two terms in the right-hand side of expression (15) correspond to the vortex force $\omega\mathbf{V}$ (see, e.g., [11]). The third term specific for He II is due to interaction between quantized vortices and the normal component.

Let us calculate the contribution from the various effects expressed by the various terms in the r.h.s. of Eq. (15). The supposition usually made in the theory superfluid turbulence is that the external superfluid velocity $\mathbf{V}_s$ is uniform. Therefore the contribution in the integral from the first term in the r.h.s. of Eq. (15) should vanish since the integral $\int \mathbf{s}'_j(\xi_j)\, d\xi_j = 0$ due to closeness of the loops.

We will show now that the contribution into vortex force due to self-induced velocity $\mathbf{V}_i$ also vanishes. Let us consider the rate of change of the Lamb impulse $\mathbf{J}_{12}$ of two loops connected with mutual induced velocity:

$$\frac{d\mathbf{J}_{12}}{dt} = -\frac{\rho_s \tilde{\kappa}^2}{4\pi} \int \mathbf{s}'_1(\xi_1)\, d\xi_1 \times \int \left(\nabla_{\mathbf{s}_1} \times \frac{\mathbf{s}'_2(\xi_2)}{|\mathbf{s}_1(\xi_1) - \mathbf{s}_2(\xi_2)|} \right) d\xi_2 - \\ -\frac{\rho_s \tilde{\kappa}^2}{4\pi} \int \mathbf{s}'_2(\xi_2)\, d\xi_2 \times \int \left(\nabla_{\mathbf{s}_2} \times \frac{\mathbf{s}'_1(\xi_1)}{|\mathbf{s}_1(\xi_1) - \mathbf{s}_2(\xi_2)|} \right) d\xi_1. \tag{16}$$

Here the ∇ operators act on the variables pointed out by the low indices. By use of the well-known formula

$$\frac{1}{|\mathbf{r}|} = \int_{\mathbf{k}} \frac{d^3\mathbf{k}}{2\pi^2 k^2} e^{i\mathbf{kr}}, \tag{17}$$

we rewrite relation (16) in the following form:

$$\frac{d\mathbf{J}_{12}}{dt} = \frac{\rho_s \tilde{\kappa}^2}{(2\pi)^3} \iiint_{\mathbf{k}} d\xi_1 d\xi_2 \frac{d^3\mathbf{k}}{\mathbf{k}^2} \exp\left[i\mathbf{k}\left(\mathbf{s}'_1(\xi_1) - \mathbf{s}'_2(\xi_2) \right) \right] \times \\ \times \left[\mathbf{s}'_1(\xi_1) \times \left(i\mathbf{k} \times \mathbf{s}'_2(\xi_2) \right) - \mathbf{s}'_2(\xi_2) \times \left(i\mathbf{k} \times \mathbf{s}'_1(\xi_1) \right) \right]. \tag{18}$$

After opening the vector production one can notice that the integrand in (18) includes combination

$$\left[\mathbf{s}'_1(\xi_1)(i\mathbf{k}\mathbf{s}'_2(\xi_2)) - \mathbf{s}'_2(\xi_2)(i\mathbf{k}\mathbf{s}'_1(\xi_1)) \right] \exp\left[i\mathbf{k}(\mathbf{s}'_1(\xi_1) - \mathbf{s}'_2(\xi_2)) \right]. \tag{19}$$

Each of the terms in Eq. (19) is the full derivative (with respect to ξ_1 and ξ_2, correspondingly) therefore the integration along each of the closed loops gives zero. For the case of the same loop the proof is almost the same.

Before we move further we have to discuss one more process governing the vortex line dynamics, namely the reconnection processes. Although there are in classical hydrodynamics (see [12]) both numerical and some analytical proofs of that the reconnection processes does not change the Lamb impulse we performed the own study of this. Our numerical data show that the Lamb impulse is indeed conserved while reconnection of lines.

The rest of the right-hand side of Eq. (15) is nothing but the force $\mathbf{F}_{sn}$ exerted by the normal component on the vortex tangle so we arrive at the following result:

$$\frac{d\mathbf{J}_V}{dt} = \mathbf{F}_{sn}. \tag{20}$$

On the one hand this result expresses the obvious fact that the rate of change of the Lamb impulse is equal to the applied external force therefore the quantity $\mathbf{J}_V$ will either vanish or grow up to infinity depending on the initial conditions. But on the other hand in steady case $\mathbf{J}_V$ should be constant and the question arises what equilibrates an action of the friction force to sustain the stationary situation.

3.3. Nonconservation of the Lamb impulse

To understand what is happening with the Lamb impulse it is instructive to follow the behavior of the single vortex ring in the counterflowing He II. If the ring is orientated along the counterflow velocity, i.e., vector $\mathbf{s}'(\xi)\times\mathbf{s}''(\xi)$ is directed along $\mathbf{V}_{ns}$ then the ring will be ballooning out reaching the side wall of the channel. The Lamb impulse of the ring is proportional to squared radius therefore process of expansion of the ring is accompanied by the increase of the quantity $\mathbf{J}_V$ and vice versa. Therefore there is the permanent motion of the vortex line elements in transverse to the counterflow direction. Since the vortex tangle as a whole has nonzero polarization along $\mathbf{V}_{ns}$ $(\langle \mathbf{s}'_j(\xi_j)\times\mathbf{s}''_j(\xi_j)\rangle = I_l\mathcal{L}_v^{1/2}\mathbf{e}$, where $\mathcal{L}_v$ is the vortex line density, $\mathbf{e}$ is unit vector in the $\mathbf{V}_{ns}$ direction) there is dominant transverse flow of the vortex line toward the side walls. Of course the situation is the same as in the vessel with particles which have some drift velocity in direction of external force, e.g., gravity. Unlike the case of the particles, which are bounced from the bottom (restoring thereby the growth of the momentum due to gravity), the vortex line annihilate at the boundaries. Together with vortex filaments the Lamb impulse associated with this particular line disappears. Process of annihilation is very involved and can be described introducing the image vortices. Besides, in the real vortex tangle the loops cannot move independently. They merge with other loops or on the contrary they break down into smaller ones. Nevertheless the main feature viz. the motion of lines to the walls and disappearing there remains valid. As for the Lamb impulse one can assert that there is permanent flux of quantity $\mathbf{J}_V$ in transverse direction. Resuming it can be stated that the steady state is nonequilibrium one with the flux both of the vortex lines (denoted further as $\mathbf{j}_{l\perp}$) and quantity $\mathbf{J}_V$ in space and the following relation between them takes place:

$$\rho_s\tilde{\kappa}\,\mathbf{j}_{l\perp} = \frac{d\mathbf{J}_V}{dt}.$$

The next conclusion which follows from the analysis given above concerns the Vinen equation for the rate $d\mathcal{L}_v/dt$ of the vortex line density. Usually only two contributions to this rate are taken into account viz. the growth of $\mathcal{L}_v$ due to mutual friction and the decay of it due to collisions of line (see, e.g., [3–5]). But our analysis asserts that there is flux of lines toward the side walls (denoted further as $\mathbf{j}_l$). The corresponding contribution may be found from relation

$$\int\limits_V \frac{d\mathcal{L}_v}{dt} d^3\mathbf{r} = -\int\limits_S \mathbf{j}_{l\perp} d^2\mathbf{r}, \qquad (21)$$

where the volume and surface integrals are taken over the whole channel. Supposing further the distribution of line inside volume is uniform and using Eq. (20) and the expression for the force $\mathbf{F}_{sn}$ (see, e.g., [3]) we obtain that the additional rate of change of the VLD due to flux toward the walls is

$$\frac{d\mathcal{L}_v}{dt} = -\alpha(I_\parallel - c_L I_l)\left|\mathbf{V}_{ns}\right|\frac{\mathcal{L}_v}{d_{\text{eff}}}. \qquad (22)$$

Here $I_\parallel, c_L, I_l$ are the structure parameters of the vortex tangle and d_{eff} is an effective size of the cross-section of the channel. It worth noting that a necessity of the additional term similar to the (22) in the Vinen equation had been discussed by Vinen himself [13]. He introduced it to adjust his experimental data and fetched some arguments to justify the particular form. From his consideration it was not clear the appearance of the channel size.

The developed consideration allows to do one more conclusion concerning the vortex tangle macroscopic dynamics. Casting Eq. (20) into standard relaxation form

$$\frac{d\mathbf{J}_V}{dt} = \frac{\delta\mathbf{F}_{sn}/\delta\mathbf{V}_{ns}}{\delta\mathbf{J}_V/\delta\mathbf{V}_{ns}}\mathbf{J}_V \qquad (23)$$

one can consider the fraction in the right-hand side of relation (23) as an estimate of the inverse relaxation time $1/\tau_j$. Accomplishing the corresponding algebraic manipulations one obtains that

$$\frac{1}{\tau_J} \approx \frac{8\alpha(1-I_{xx})}{\beta}\mathbf{V}_{ns}^2. \qquad (24)$$

Thus the time of relaxation of the Lamb impulse is of order of the one for the vortex line density dynamics (see, e.g., [5]). But that implies that macroscopic description of the vortex tangle cannot be restricted by the only Vinen equation but should include as well equation for the Lamb impulse.

4. The dynamics of an inhomogeneous quantum turbulence

4.1. Diffusion of the vortex tangle

Method of the trial distribution function allowed us to study a problem of dynamics of an inhomogeneous vortex tangle. An attempt to describe these processes was made in [14,15], where the term $D_v\nabla^2 L(r,t)$ (here L is the vortex line density) was introduced into the Vinen equation. The authors were not able to restore the value of the diffusion coefficient D_v from experimental data (these results are reviewed and discussed in [5]). Both the diffusion process and the diffusion coefficient we obtained from the so-called nonequilibrium thermodynamics principles developed by Jou, Mongiovi, and Sciacca in a series of works (see, e.g., [16,17] and references therein). The described works were pure phenomenological approaches without relation to the vortex loops motion. In paper [18] the spatial diffusion of an inhomogeneous vortex tangle had been studied numerically. Analyzing their results, the authors determined the diffusion constant to be of the order of 0.1κ. Barenghi and Samuels [19] has studied evaporation of the vortex loops from the inhomogeneous vortex tangle numerically. However, since the authors studied the dilute tangle, they observed the “ballistic” regime, rather than pure diffusion [19].

The quantitative theory of the diffusion-like spreading of the VT was developed by the author; details can be found in paper [20]. The study is based on the TDF method stated in Sec. 2. Vortex loops composing the vortex tangle can move as a whole with a drift velocity V_l depending on their structure and their length. The flux of the line length, energy, momentum etc. executed by the moving vortex loops takes place. In the case of inhomogeneous vortex tangle the net flux $\mathbf{J}$ of the vortex length due to the gradient of concentration of the vortex line density $\mathcal{L}(x,t)$ appears. The situation here is exactly the same as in the classical kinetic theory with the difference being that the “carriers” are not the point particles but the extended objects (vortex loops), which themselves possess an infinite number of degrees of freedom with very involved dynamics. It is possible to fulfill investigation basing on the supposition that vortex loops have the Brownian or random walk structure with the generalized Wiener distribution (Sec. 2). To develop the theory of the transport processes fulfilled by vortex loops (in the spirit of classical kinetic theory) we need to calculate the drift velocity V_l and the free path $\lambda(l)$ for the loop of size l. Referring to the paper [20] we write down here the following result. The drift velocity V_l for the loop of size l is

$$V_l = C_v \beta / \sqrt{l \xi_0}. \tag{25}$$

Quantity C_v is numerical factor of the order of unity. The free path $\lambda(l)$ for loop of length l is

$$\lambda(l) = 1/2lb_m\mathcal{L}. \tag{26}$$

Here b_m is the numerical factor approximately equal to $b_m \approx 0.2$. It is seen that free path $\lambda(l)$ is very small, implying that only very small loops give a significant contribution to transport processes, e.g., loop of the size equal to the interline space $\delta = \mathcal{L}^{-1/2}$ can fly (in average) about 2–3 times δ distance. However, when the vortex tangle becomes dilute enough, the larger loops can fly the distance comparable with the size of the bulk.

Knowing the averaged velocity V_l (l) of loops, and the free path $\lambda(l)$ (both quantities are l-dependent) we can evaluate the spatial flux of the vortex line density $\mathcal{L}$ executed by the loops. The procedure is very close to the one in the classical kinetic theory, with the difference being that the carriers have different sizes, requiring additional integration over the loop lengths. Let us consider the small area element placed at some point x, and oriented perpendicularly to axis x. The x component flux of the line length executed by loops of sizes l, placed in θ, φ direction (from the left and right sides, correspondingly), and remote from the area element at distance R, can be written as

$$d\mathbf{j}_{\mp}(\theta, \varphi, l, R) = ln(l, R, \theta, \varphi)(V_l \cos\theta) P(R), \tag{27}$$

where $V_l \cos\theta$ is just the x component of the drift velocity, the factor $P(R)$ is introduced to control an attenuation of flux, due to collisions. We took the density of loops $n(l)$ and, accordingly, vortex line density $\mathcal{L}$, both of which are functions of space variable (in spatial spherical coordinates $n = n(l, R, \theta, \varphi)$, $\mathcal{L} = \mathcal{L}(l, R, \theta, \varphi)$). In the spirit of classical kinetic theory, we assume the local equilibrium is established. Performing all prescribed computations (see for details [20]) we write the flux $\mathbf{J}$ of vortex line is proportional to $\nabla\mathcal{L}$, $\mathbf{J} = D_v \nabla\mathcal{L}$ and, correspondingly, the spatial-temporal evolution of quantity $\mathcal{L}$ obeys the diffusion-type equation

$$\frac{\partial \mathcal{L}}{\partial t} = D_v \nabla^2 \mathcal{L}. \tag{28}$$

Our approach is fairly crude to claim a good quantitative description. However, if we were to adopt the data grounded on the results of the theory described in [20,21] it is possible to conclude that $D_v \approx 2.2\kappa$. The diffusion-like evolution of the vortex tangle on the base Eq. (28) satisfactory describes the decay of quantum turbulence (see [20]).

4.1.1. Propagation of the turbulent fronts. One more application of the Gaussian model, which we would like to review here, is the problem of the propagation of a turbulent superfluid domain (see paper by the author [22]). This phenomenon was observed in many experiments, from the quantum turbulence created by the heat load [14,15,23] up to turbulent front of uniform vorticity in a rotating ^{3}He [24,25]. A key assumption is that the propagation of the front occurs in the manner of a diffusion, with the source of the vortices behind the front. In the one-dimensional case (when the front propagates along the x axis) equation for the vortex line density is

$$\frac{\partial \mathcal{L}(t,x)}{\partial t} + \frac{\partial \mathcal{L}(t,x) V_L}{\partial x} = D \frac{\partial^2 \mathcal{L}(t,x)}{\partial x^2} + F(\mathcal{L}(t,x)). \tag{29}$$

In the case of the counterflowing turbulence, the source term is just the right-hand side of the Vinen equation

$$F_{\mathrm{Vi}}(\mathcal{L}) = \alpha_{\mathrm{Vi}}\left|\mathbf{v}_{ns}\right|\mathcal{L}^{3/2} - \beta_{\mathrm{Vi}}\mathcal{L}^{2}. \tag{30}$$

An analysis performed in the spirit of combustion theory (see, e.g., [26]) leads to a formula for the propagation speed V_{fr} of the front:

$$V_{\mathrm{fr}} = 0.8\sqrt{D/\tau_V}. \tag{31}$$

Here D is the diffusion coefficient and τ_V is the relaxation time of the vortex tangle. For the pure counterflowing turbulence, the diffusion constant is about $D_v \approx 2.2\kappa$ (see Eq. (28)) and relaxation time τ_V can be taken from Eq. (30):

$$\tau^{-1}(\mathcal{L}) = \beta_{\mathrm{Vi}}\mathcal{L}_{\mathrm{eq}}. \tag{32}$$

Result (31) agrees perfectly with the classical Peshkov–Tkachenko experiment [23], who studied the kinetics of formation of the superfluid turbulence in long capillaries under the influence of small heat fluxes, of the order of $1\ \mathrm{W/cm}^2$. They reported the velocity of front $V_{\mathrm{exp}} \approx 0.27\ \mathrm{cm/s}$, whereas Eq. (31) gives $V_{\mathrm{theor}} \approx 0.23\ \mathrm{cm/s}$.

5. Conclusion

We briefly exposed an essence of the method of trial distribution function, or Gaussian model in theory of quantum turbulence, and give several examples how it can be used for evaluation of important physical characteristics such as induced momentum and the vortex loops diffusion. These characteristics has been discussed early (see, e.g., [4]), however their evaluation has not been performed because of lack of a proper theory. We think that these illustrations convince that Gaussian model can serve as effective tool to study chaotic vortex filaments. There are other important applications of the trial distribution function enables us to develop theory of colliding loops, they are stated in original papers by the author [21,27,28] and will be reviewed in Physical Reports.

Acknowledgments

The work was supported by the grants N 10-08-00369 and N 10-02-00514 from the Russian Foundation of Basic Research, and by the grant from the President Federation on the State Support of Leading Scientific Schools NSh-6686.2012.8.

1. W. Vinen, *J. Low Temp. Phys*. **161**, 419 (2010).
2. L. Skrbek and K.R. Sreenivasan, *Phys. Fluids* **24**, 011301 (2012).
3. K.W. Schwarz, *Phys. Rev. B* **38**, 2398 (1988).
4. R. Donnelly, *Quantized Vortices in Helium II*, Cambridge University Press, Cambridge, UK (1991).
5. S.K. Nemirovskii and W. Fiszdon, *Rev. Mod. Phys*. **67**, 37 (1995).
6. M. Doi and S. Edwards, *The Theory of Polymer Dynamics*, Clarendon, Oxford (1986).
7. S.K. Nemirovskii, *Phys. Rev. B* **57**, 5972 (1998).
8. G. Batchelor, *An Introduction to Fluid Mechanics*, Cambridge University Press, Cambridge, England (1967).
9. S.K. Nemirovskii, *Phys. Rev. B* **57**, 5987 (1998).
10. F. Vidal and D. Lhuillier, *Phys. Rev. B* **13**, 148 (1976).
11. P. Saffman, *Vortex Dynamics*, Cambridge University Press, Cambridge, England (1992).
12. A.K.M.F. Hussain, *J. Fluid Mechanics* **173**, 303 (1986).
13. W. Vinen, *Proc. R. Soc. Lond, Ser. A* **242**, 493 (1957).
14. H. van Beelen, W. van Joolingen, and K. Yamada, *Physica B: Condens. Matter* **153**, 248 (1988), ISSN 0921-4526.
15. J.A. Geurst, *Physica A* **154**, 280 (1992).
16. D. Jou, M. Mongiovi, and M. Sciacca, *Physica D* **240**, 249 (2011).
17. M.S. Mongiovi, D. Jou, and M. Sciacca, *Phys. Rev. B* **75**, 214514 (2007).
18. M. Tsubota, T. Araki, and W.F. Vinen, *Physica B*: *Condens. Matter* **329**–**333**, 224 (2003).
19. C.F. Barenghi and D.C. Samuels, *Phys. Rev. Lett*. **89**, 155302 (2002).
20. S.K. Nemirovskii, *Phys. Rev. B* **81**, 064512 (2010).
21. S. K. Nemirovskii, *Phys. Rev. B* **77**, 214509 (2008).
22. S. Nemirovskii, *J. Low Temp. Phys*. **162**, 347 (2011), ISSN 0022-2291).
23. V.P. Peshkov and V.K. Tkachenko, *Sov. Phys. JETP* **14**, 1019 (1961).
24. V. Eltsov, R. de Graaf, R. Hanninen, M. Krusius, R. Solntsev, V. L'vov, A. Golov, and P. Walmsley, in *Progress in Low Temperature Physics: Quantum Turbulence* Elsevier (2009), vol. 16, p. 45.
25. J.J. Hosio, V.B. Eltsov, R. de Graaf, P.J. Heikkinen, R. Hanninen, M. Krusius, V.S. L'vov, and GE. Volovik, *Phys. Rev. Lett*. **107**, 135302 (2011).
26. D.A. Frank-Kamenetskii, *Diffusion and Heat Exchange in Chemical Kinetics*, Princeton Univ. Press, Princeton, NJ (1955).
27. S.K. Nemirovskii, *Phys. Rev. Lett*. **96**, 015301 (2006).
28. S. Nemirovskii, *J. Low Temp. Phys*. **142**, 769 (2006).